Microchimica Acta (2019) 186:709
https://doi.org/10.1007/s00604-019-3857-z

ORIGINAL PAPER

Electrochemical lead(II) biosensor by using an ion-dependent split DNAzyme and a template-free DNA extension reaction for signal amplification

Li Zhang[1] · Hanmei Deng[1] · Ruo Yuan[1] · Yali Yuan[1]

Received: 12 May 2019 / Accepted: 19 September 2019

Abstract

A voltammetric biosensor for lead(II) (Pb^{2+}) is described that is based on signal amplification by using an ion-dependent split DNAzyme and template-free DNA extension reaction. The Pb^{2+}-dependent split DNAzyme was assembled on gold nanoparticles (Au@Fe_3O_4), and this nanoprobe then was exposed to Pb^{2+} which causes the split-off of DNAzymes to release primers containing 3′-OH groups (S_1 and S_2). The template-free DNA extension reaction triggers the generation of long ssDNA nanotails, which then can bind the free redox probe N,N′-bis(2-(trimethylammonium iodide)propylene)perylene-3,4,9,10-tetracarboxyldiimide (PDA^+) via electrostatic adsorption. Hence, the concentration of PDA^+ in solution is reduced. Therefore, less free PDA^+ can be immobilized on a glassy carbon electrode modified with electrodeposited gold nanoparticles (depAu) to produce an electrochemical signal, typically measured at ~0.38 V (*vs.* SCE) for quantitation of Pb^{2+}. The use of a Pb^{2+}-dependent split DNAzyme avoids the usage of a proteinic enzyme. It also increases the sensitivity of the sensor which has a lower detection limit of 30 pM of Pb^{2+}.

Keywords Long ssDNA nanotails · Electrostatic adsorption · Sensitive detection · Electrochemical biosensor

Introduction

Lead ions (Pb^{2+}) are a common environmental pollutant accompanied by severe human health risks [1–3]. It was demonstrated that Pb^{2+} can react with the sulfhydryl groups of enzymes. It also can become a substitute of essential metal ions such as iron(III), calcium(II) and zinc(II). This can cause acute and chronic illnesses including colic-like abdominal pains and nephropathy [4]. According to the standard of U.S. environmental Protection Agency (EPA) and World Health Organization (WHO), the maximum acceptable amount of lead in drinking water are 50 μg/L and 10 μg/L, respectively [5, 6]. It is therefore of great importance to explore new approaches to achieve the ultrasensitive detection of Pb^{2+}.

Recently emerging Pb^{2+}-dependent split DNAzyme, a DNA nanostructure composed by a catalytic DNA strand (Cat) and a ribonucleobase-containing substrate DNA strand (Sub) [7], can be specially cleaved by Pb^{2+} with high cleavage activity for releasing massive small DNA segments and thus provide a possibility for its application in the on-site Pb^{2+} analysis. Based on this, many biosensors with the usage of different detection techniques, including surface-enhanced raman scattering (SERS) [8, 9], fluorescence [10], colorimetry [11], electrochemiluminescence (ECL) [12] and electrochemistry (EC) [13, 14], have been fabricated for implementing the Pb^{2+} analysis. Among them, EC based analysis systems showed desirable advantages of cost-effective procedure, simple operation and miniaturization, and thereby have received considerable attention [15].

The DNA amplification technologies, such as enzyme-assisted recycle cleavage [16, 17], strand displacement amplification [18, 19] and DNA extend reaction [20], are effective ways to improve the detection sensitivity of biosensors. Especially, the DNA extend reaction with the unique property of producing long single or double stranded DNA (ssDNA/dsDNA) nanotails exhibits desiring advantages in

✉ Yali Yuan
y198688@swu.edu.cn

[1] Key Laboratory of Luminescent and Real-Time Analytical Chemistry, Ministry of Education, College of Chemistry and Chemical Engineering, Southwest University, Chongqing 400715, People's Republic of China

Published online: 24 October 2019

biosensing applications, through which different massive signal probes or enzymes can be decorated simply and quickly. However, traditional DNA extend approaches, including rolling circle amplification (RCA) [21, 22], hybridization chain reaction (HCR) [23, 24], exponential amplification reaction (EXPAR) [25–27], polymerase chain reaction (PCR) [28] and loop-mediated isothermal amplification (LAMP) [29, 30], were driven by DNA templates and required strict base pairing, making the systems suffered from not only structural complexity but also fussy operation. Fortunately, the template-free DNA extension reaction, in which the consecutive addition of deoxyribonucleoside 5′-triphosphates (dNTP) at 3′-OH group of DNA is effectively catalyzed by terminal deoxynucleotidyl transferase (TdT) [31, 32], can resolve the above-mentioned problems to a certain extent. The entirely extension reaction process need no DNA template, and thus the DNA sequence can be easily designed and operated, thereby providing a simple, direct and efficient isothermal amplification method for producing long ssDNA nanotails in construction of ultrasensitive biosensors.

The redox probes N,N′-Bis(2-(trimethylammonium iodide)propylene) perylene-3,4,9,10-tetracarboxyldiimide (PDA^+), a derivative of 3,4,9,10-perylene- tetracarboxylic dianhydride, possesses the positive charges at both ends, which can be decorated on negative charged DNA or gold nanoparticles (depAu) via electrostatic adsorption. Moreover, the PDA^+ is an aromatic molecule consisting of five phenyl rings structure and two imides at both end of perylene molecule, which possesses superior electro/optical property. Therefore, the PDA^+ was used as redox probe and first applied in construction of electrochemical biosensor. In this work, by combining Pb^{2+}-dependent split DNAzyme with temple-free DNA extension reaction, a simple and ultrasensitive EC-biosensor was designed for determination of Pb^{2+}. The Pb^{2+}-dependent split DNAzyme assembled on Au@Fe_3O_4 (nanoprobes) was first subjected to the target Pb^{2+}. Here, the Pb^{2+} can specially split DNAzymes to release substantial primers containing 3′-OH group (S_1 and S_2), and thus trigger the temple-free DNA extension reaction to generate amounts of long ssDNA nanotails, on which a lots of free redox probes PDA^+ were decorated via electrostatic adsorption. Since the PDA^+ in tube was at a constant total, the decoration of PDA^+ on long ssDNA nanotails would lead to the reduce of free PDA^+ in solution, leaving few free PDA^+ for being immobilized on depAu modified electrode (depAu/GCE) to produce low EC signal for quantitative detection of Pb^{2+}. The Pb^{2+}-dependent split DNAzyme not only avoided the usage of enzyme label, but also effectively increased the sensitivity of proposed biosensor, providing a simple and sensitive strategy for Pb^{2+} analysis.

Experimental

Chemicals and reagents

Chloroauric acid ($HAuCl_4$), silver nitrate ($AgNO_3$), hexanethiol (HT), Fe_3O_4 magnetic nanoparticles (Fe_3O_4), Zinc nitrate ($Zn(NO_3)_2$), phthalic diglycol diacrylate (PDDA) and tris(hydroxymethyl)aminomethane (Tris) were purchased from Sigma (St. Louis, MO, USA) (http://www.sigmaaldrich.com). 3,4,9,10-perylenetetr- acarboxylic dianhydride (PTCDA) used for synthetizing N,N′-Bis(2-(trimethylammonium iodide)propylene)perylene-3,4,9,10-tetracarboxyl- diimide (PDA^+) was supplied from Lian Gang Dyestuff Chemical Industry Co. Ltd. (Liaoning, China) (http://www.lyliangangdyes.com). Terminal deoxynucleotidyl transferase (TdT) and its buffer containing 1 M potassium cacodylate, 0.05% (*V*/*V*) Triton X-100, 5 mM $CoCl_2$, and 0.125 M Tris, pH 7.2) were supplied from Beyotime Biotech Co. Ltd. (Nantong, China) (https://www.beyotime.com/index.htm). The catalytic strand (Cat): 5′-SH-$(CH_2)_6$-CAT CTC TTC TCC GAG CCG GTC GAA ATA GTG AGT-3′ and substrate strand (Sub): 5′-GTG GAT TTA GGG TGA GGT GAG TGA GAC TCA CTA TrA GGA AGA GAT GGG TAG GAG TGG GAT GAG GAT TTG G-3′, and deoxyadenosine triphosphate (dATP) were all supplied from Sangon Biotech Co. Ltd. (Shanghai, China) (https://www.sangon.com). All aqueous solutions were prepared with ultrapure water (18.2 MΩ·cm, MilliQ, Millipore).

Apparatus

All electrochemical measurements were conducted on a computer controlled CHI 660E electrochemical system (Shanghai Chenhua Instrument, China) with a traditional three-electrode system. The differential pulse voltammetric (DPV) signals were recorded in 0.10 M phosphate buffered solution (PBS, pH 7.0) containing 0.1 M Na_2HPO_4, 0.1 M KH_2PO_4, and 0.1 M KCl. The parameters were listed as follows, potential: −0.6 to 0 V; modulation amplitude: 0.05 V; pulse width: 0.05 s and sample width: 0.0167 s. The cyclic voltammetry (CV) was performed with the potential ranged from −0.2 V to 0.6 V at 100 mV s^{-1} in 0.10 M PBS (pH 7.0) containing 5 mM $[Fe(CN)_6]^{3-/4-}$. The electrodeposition of depAu was performed in 1 *wt*% $HAuCl_4$ solution with the usage of constant potential of −0.2 V and reaction for 30 s.

Synthesis of PDA^+ redox probes

The synthesis procedure of redox probe PDA^+ is listed as follows: 1.5 mL 3-dimethylaminopropylamine (118 mM) and 0.5 g PTCDA (12.1 mM) were added into 20 mL isobutanol and reacted for 24 h at 90 °C under stirring. After filtering, the raw product was subjected to NaOH solution at 80 °C for

reaction of 30 min for removing superfluous PTCDA, followed by washing with the usage of ethanol and deionized water, respectively. After drying under vacuum, 0.3 g raw product, 0.15 mL ethyl iodide and 15 mL toluene were added into a round bottom flask equipped with a stirring condenser and refluxed for 3 h. At the conclusion of the reaction, the mixture was cooled to room temperature and filtered. Then, the aether was used to wash the precipitate. After drying under vacuum, brownish red PDA^+ thus acquired for further use.

Synthesis of Pb^{2+}-dependent DNAzyme decorated $Au@Fe_3O_4$ nanoprobes

2 mg mL^{-1} Fe_3O_4 magnetic nanoparticles (Fe_3O_4) were first washed three times by ultrapure water. Then, the washed Fe_3O_4 was subjected to 1 mL 0.2 *wt*% PDDA solution for reaction at room temperature for 30 min. Afterwards, 5 mL gold nanoparticles (Au) solution prepared according to the literature [33] was added into above mixture. Since the PDDA possessed the positive charges, the Au with negative charges can be successfully assembled on PDDA functional Fe_3O_4 surface via electrostatic adsorption. After incubation overnight at room temperature with gentle shaking, the residual Au was moved by using magnetic separation. Following that, the precipitate ($Au@Fe_3O_4$ nanoparticles) was redispersed in 6 mL PBS. Then, 50 μL Pb^{2+}-dependent DNAzyme (Cat and Sub, 50 μM, respectively) was added into 1 mL prepared $Au@Fe_3O_4$ solution and reacted half one day at 4 °C. To block the nonspecific binding sites on Au, 200 μL HT (50 mM) was dropped into the solution and reacted 40 min. After magnetic separation, the final Pb^{2+}-dependent DNAzyme decorated $Au@Fe_3O_4$ nanoprobes was redispersed in 1 mL PBS for further use.

Principle of electrochemical DNA biosensor for Pb^{2+} detection

The principle of proposed electrochemical biosensor based on Pb^{2+}-dependent DNAzyme cleavage recycling and template-free DNA extension reaction is shown in Fig. 1. The 10 μL

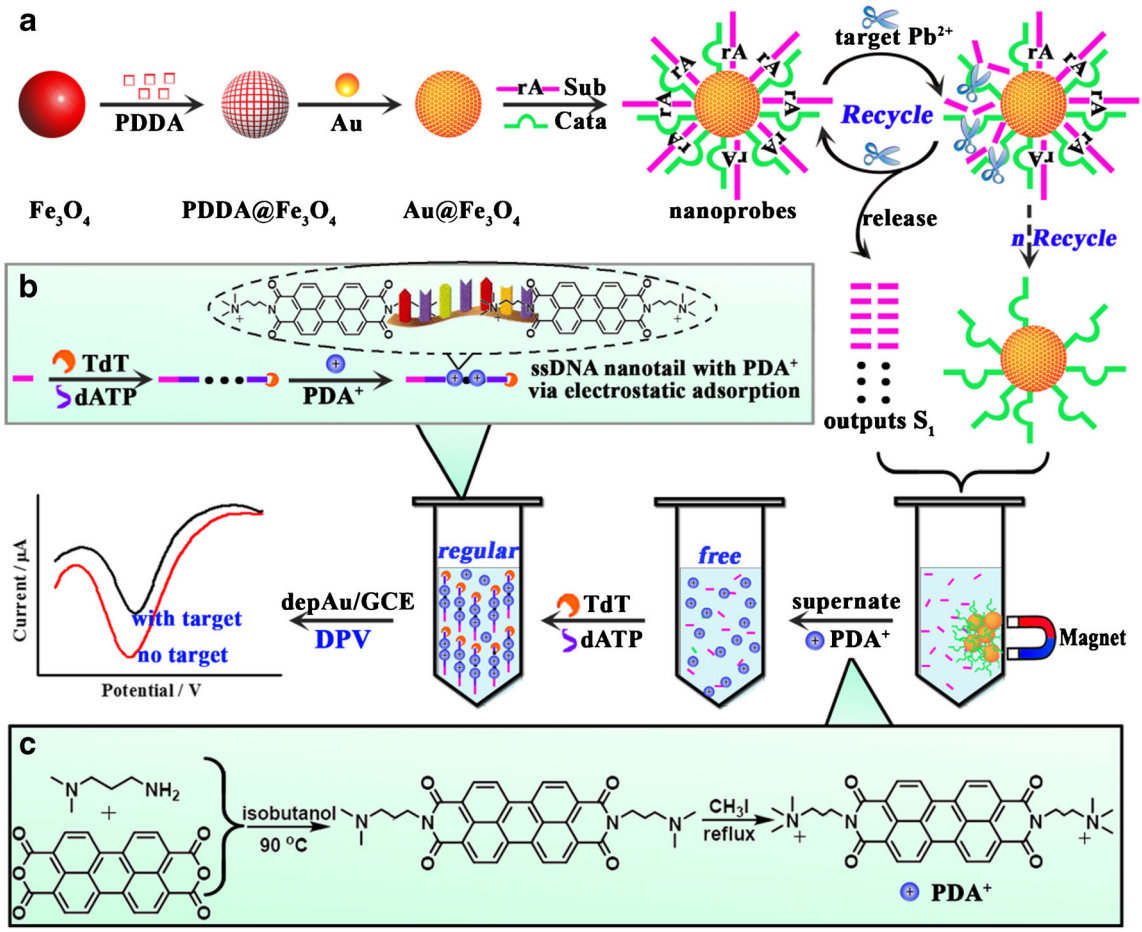

Fig. 1 Schematic illustration of the electrochemical aptasensor for Pb^{2+} analysis based on ion-dependent DNAzyme cleavage recycling and DNA extension reaction: (a) the principle of electrochemical DNA biosensor for Pb^{2+} detection; (b) the formation of long ssDNA nanotail; (c) the synthesis route of PDA^+

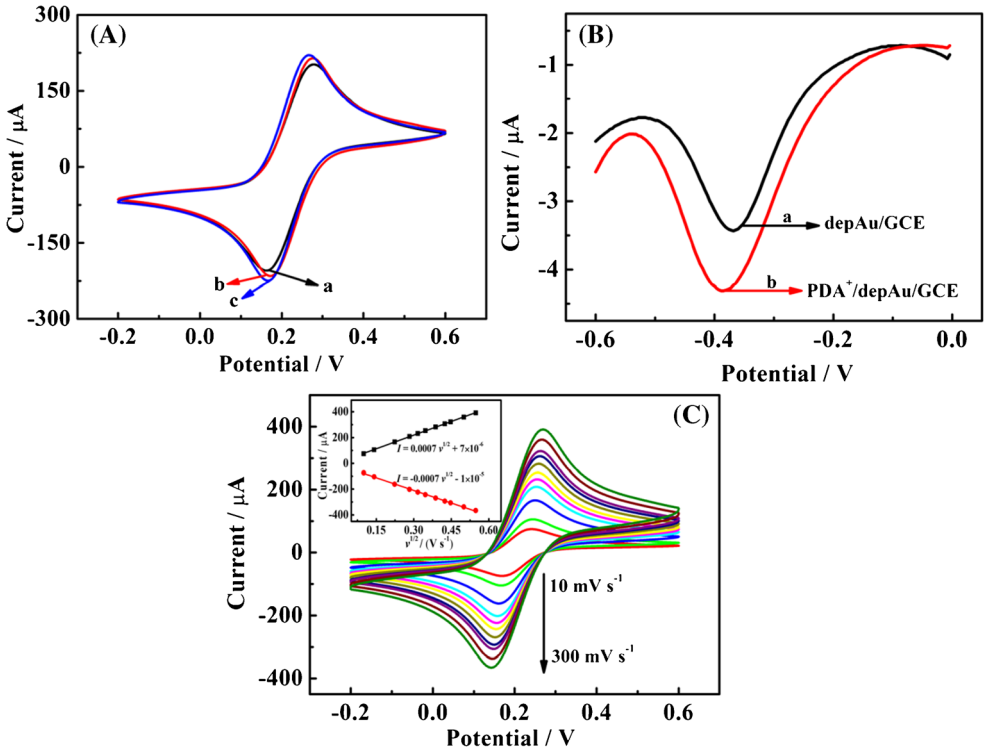

Fig. 2 (A) CVs of bare GCE (a), depAu/GCE (b) and PDA^+/depAu/GCE (c) investigated in 0.10 M PBS (pH 7.0) containing 5 mM $[Fe(CN)_6]^{3-/4-}$. (B) DPV responses of depAu/GCE (a) and PDA^+/depAu/GCE (b) investigated in 0.10 M PBS (pH 7.0). (C) The CVs of Au/GCE in 0.10 M PBS (pH 7.0) containing 5 mM $[Fe(CN)_6]^{3-/4-}$ with different sweep rates: 10, 20, 50, 80, 100, 120, 150, 180, 200, 250 and 300 mV s^{-1}. The inset shows the dependence of redox peak currents on the square root of scan rate

target Pb^{2+} with different concentrations was first subjected to 20 μL prepared Pb^{2+}-dependent DNAzyme decorated $Au@Fe_3O_4$ nanoprobes solution for reaction of 40 min. Through the Pb^{2+}-dependent DNAzyme cleavage recycling amplification, the small amount of target Pb^{2+} was converted into numerous 3′-OH output DNAs (S_1), which thus further triggered the DNA extension reaction to directly generate the long ssDNA. Therefore, after the magnetic separation, 10 μL TdT extension solution (200 UmL 1^{-1} TdT, 2.5 mM $CoCl_2$ and 10 mM dATP) was added into the supernatant and reacted at 37 °C for 60 min. Subsequently, a fixed concentration of 4 μL 0.3 μM PDA^+ with positive charges was adopt into solution for its adsorption on negative charged long ssDNA nanotail, resulting in the reduce of free PDA^+ in solution. Then, the solution was coated on depAu modified electrode for incubation of 40 min. Owing to the depAu/GCE can capture the free PDA^+, a detectable electrochemical signal was acquired for quantitative detection of Pb^{2+}.

Results and discussion

Electrochemical characterization of the modified electrode

The CV was used to monitor the sequential fabrication of the modified electrodes, including the modification of depAu and free PDA^+ on electrode. And all the electrodes were investigated in 0.10 M PBS (pH 7.0) containing 5 mM $[Fe(CN)_6]^{3-/4-}$ and the corresponding results were displayed in Fig. 2A. As expected, because of the excellent redox activity of $[Fe(CN)_6]^{3-/4-}$, a couple of redox peak is acquired (curve a). Owing the superior conductivity of depAu, an increase in peak current can be observed after the modification of depAu on electrode (curve b). Likewise, the absorption of PDA^+ on electrode can lead to a further increase in peak current (curve c), this is because that the PDA^+ with positive charges can facilitate the electron transfer

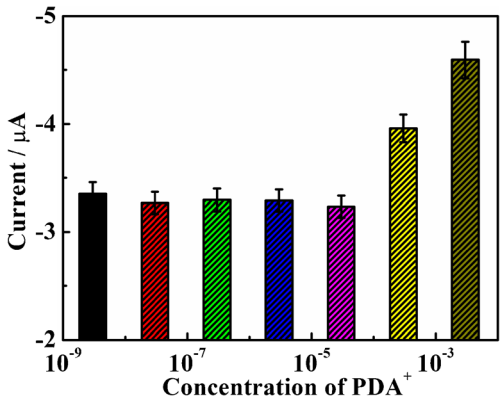

Fig. 3 Effect of PDA^+ concentrations on the sensor performance (target Pb^{2+} was set at 10 nM). Error bars represent standard deviations of three parallel experiments

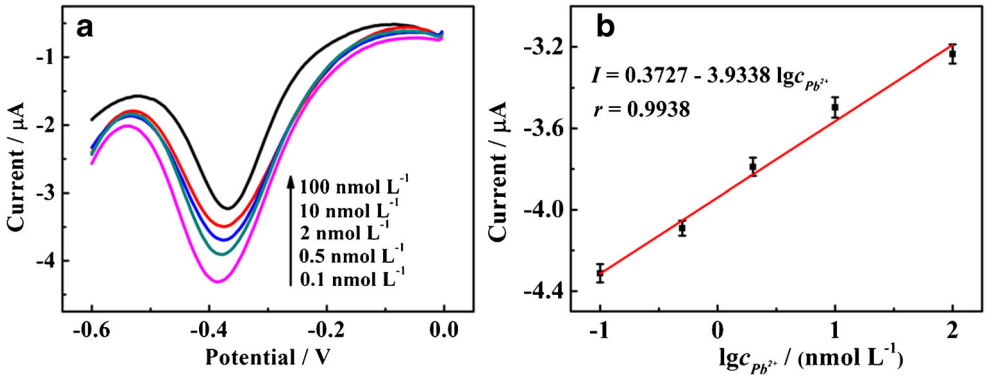

Fig. 4 (A) DPV responses of proposed biosensor in response to devise target-Pb^{2+} concentrations (0.1, 0.5, 2, 10 and 100 nM); (B) Calibration plot for the electrochemical signals against the logarithm of target-Pb^{2+} concentrations ranging from 0.1 nM to 100 nM

on electrode. Moreover, the DPV was also used for testifying the successful immobilization of PDA^+ on electrode. Here, the 0.10 M PBS (pH 7.0) was served as detection buffer. It can be seen from Fig. 2B that the PDA^+/depAu/GCE (curve b) have an obvious peak current compared to that of depAu/GCE (curve a), indicting the feasibility of proposed approach.

Additionally, the CV responses of Au/GCE using different scan rate, including 10, 20, 50, 80, 100, 120, 150, 180, 200, 250 and 300 mV s^{-1} were also investigated. The 0.10 M PBS (pH 7.0) containing 5 mM $[Fe(CN)_6]^{3-/4-}$ was used as the detection buffer. From the results we can see that, the both anodic and cathodic peak currents increased linearly with the square root of scan rate between 10 and 300 mV s^{-1}, suggesting a diffusion-controlled process of the $[Fe(CN)_6]^{3-/4-}$ couple at the modified electrode. The results are shown in Fig. 2C. Additionally, the electroactive surface area of the Au/GCE was studied by CV in 5 mM $[Fe(CN)_6]^{3-/4-}$ at different sweep rates using the Randles-Sevcik equation:

$$I_p = \left(2.69 \times 10^5\right) n^{3/2} A D_o^{1/2} C_o v^{1/2}$$

in which D_o is the standard diffusion coefficient of $[Fe(CN)_6]^{3-/4-}$, I_p is the measured current maximum, n is the number of electrons, C_o is concentration of analyte, and ν is the sweep rate. As a result, the electroactive surface area of the Au/GCE is 0.165 cm^2.

Optimization of the PDA^+ concentration

As mentioned above, a fixed concentration of PDA^+ with positive charge was need to be adopt into the solution containing amounts of formed long ssDNA nanotail. Except for the PDA^+ absorbed on long ssDNA nanotail, there also retained some free PDA^+ used for immobilizing on depAu/GCE for generating detectable electrochemical signal. Thus, the initial concentration of PDA^+ was a key factor in the performance of proposed biosensor. Obviously, superfluous PDA^+ led to a high background signal while inadequate PDA^+ might bring in the very low detection signal and detection range, thereby influencing the detection sensitivity to a certain extent. Accordingly, the concentration of PDA^+ was optimized here. Concentrations of PDA^+ ranged from 3×10^{-9} to 3×10^{-3} M was selected here. The results in Fig. 3 displays that the detection system have no obviously signal change in the range from 3×10^{-9} to 3×10^{-5} M, however, when the concentrations of PDA^+ reach to 3×10^{-4} M, an obviously change in the

Table 1 Comparison of the proposed sensing system with other reported works using different methods for Pb^{2+} detection

Analytical method	Materials used	Linear range	Detection limit	Ref.
Fluorescence	graphene quantum dots and gold nanoparticles	10 pM - 50 nM	5.6 pM	34
Spectrophotometric	unimolecular peroxidase-like deoxyribozyme	0.05 μM - 1.2 μM	27 nM	35
Colorimetric	glutathione functionalized gold nanoparticles	0.1 μM - 50 μM	100 nM	36
Electrochemical	nitrogendoped graphene/chitosan nanocomposite	0.1 μM - 100 μM	66.4 nM	37
Colorimetric	colloidal gold nanoparticles	0 nM - 15 nM	59.39 pM	38
Fluorescence	ion imprinted fluorescence polymers	0.1 μM - 5.0 μM	34 nM	39
Electrochemical	DNA functionalized porphyrinic metal-organic framework	0.05 nM - 200 nM	34 pM	40
Electrochemical	3D DNA-gold nanoparticles network	100 pM - 5 μM	95 pM	41
pH meter	Pb^{2+}-specific DNAzyme immobilized magnetic beads	1.0 nM – 100 nM	0.91 nM	3
Colorimetric	Pb(II)-binding aptamer immobilized gold nanoparticles	10 nM – 1.5 μM	2.4 nM	42
Fluorometric	DNAzyme modified graphene oxide	0 nM - 3 nM	96 pM	43
Electrochemical	Pb^{2+}-dependent DNAzyme decorated gold nanoparticles@Fe_3O_4	0.1 nM - 100 nM	30 pM	This work

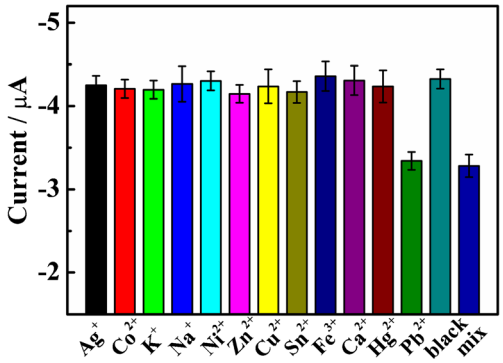

Fig. 5 Selectivity analysis of the biosensor (100 nM Ag^{+}; 100 nM Co^{2+}; 100 nM K^{+}; 100 nM Na^{+}; 100 nM Ni^{2+}; 100 nM Zn^{2+}, 100 nM Cu^{2+}, 100 nM Sn^{2+}, 100 nM Fe^{3+}, 100 nM Ca^{2+}, 100 nM Hg^{2+}, 10 nM Pb^{2+}; blank and the mixture containing 100 nM Cu^{2+}, 100 nM Sn^{2+}, 100 nM Fe^{3+}, 100 nM Ca^{2+}, 100 nM Hg^{2+} and 10 nM Pb^{2+}). Error bars represent the standard deviation from four independent experiments

DPV signal can be acquired and the current continuously increase with the increasing concentration. Therefore, the optimized PDA^{+} concentration is 3×10^{-5} M.

Performance of biosensor for determination of Pb^{2+}

Under the optimized conditions, the DPV responses at devise concentrations of Pb^{2+} were measured. As displayed in Fig. 4A, the DPV signal decrease with the increase of Pb^{2+} concentration, suggesting that more Pb^{2+} used for recycling cleavage of ion-dependent DNAzyme, the more DNA fragments acquired to produce substantial DNA long ssDNA nanotail for PDA^{+} immobilization, effectively reduces the residual free PDA^{+} in solution for assembling on depAu/GCE. After repeated trials ($n = 3$), the average decrease of the peak values shows a good relationship toward the logarithm of Pb^{2+} concentration in the range of 0.1 ~ 100 nM (Fig. 4B). The corresponding regression equation is $I = 0.3727–3.9338 \lg c_{Pb}{}^{2+}$ and a calculated detection limit is 30 pM. From the results we can see that the proposed approach displays a relative wide linear detection range and low detection limit, suggesting that the designed target-induced cleavage recycling and rolling circle amplification (RCA) can effectively improve the sensitivity of proposed biosensor. Moreover, the property of proposed sensing system is compared with that of some reported works. From the Table 1, we can see that the proposed biosensor shows desiring liner range and detection limit, providing a sensitive approach for Pb^{2+} detection.

Table 2 Recovery Experiments of Pb^{2+} in Drinking Water Samples

Samples	Added Pb^{2+}/nM	Found Pb^{2+}/nM	Recovery/ %	RSD/ %
1	0.5	0.48	96.2	4.3
2	2	2.05	102.5	4.5
3	10	9.65	96.5	4.8
4	100	103.5	103.5	5.2

Table 3 Detection of tap water samples containing defined Pb^{2+} concentration by atomic absorption spectrometry (AAS) using proposed biosensor ($n = 3$)

Proposed Biosensor (nM)				AAS (nM)			
1	2	3	RSD	1	2	3	RSD
90.2	97.7	99.8	5.3%	96.6	103.5	99.3	3.5%

Selectivity and reproducibility

The selectivity test of proposed electrochemical biosensor toward several different ions (including Ag^{+}, Co^{2+}, K^{+}, Na^{+}, Ni^{2+}, Zn^{2+} Cu^{2+}, Sn^{2+}, Fe^{3+}, Ca^{2+} and Hg^{2+}) was also conducted. As shown in Fig. 5, only a distinct change of electrochemical response toward Pb^{2+} can be obtained when compared with other ions even the concentration up to 10-fold. Moreover, the cross-sensitivity to other species were also investigated, the sample containing 10 nM Pb^{2+}, 100 nM Cu^{2+}, 100 nM Sn^{2+}, 100 nM Fe^{3+}, 100 nM Ca^{2+} and 100 nM Hg^{2+} was also detected here. As shown in Fig. 5, the electrochemical signal of biosensor towards sample containing 10 nM Pb^{2+}, 100 nM Cu^{2+}, 100 nM Sn^{2+}, 100 nM Fe^{3+}, 100 nM Ca^{2+} and 100 nM Hg^{2+}, is approximated to the current of biosensor towards sample containing 10 nM Pb^{2+} only. These results suggest that the co-exist of other interferences would not influence the detection of Pb^{2+}, suggesting that the electrochemical detection of Pb^{2+} with this biosensor is highly selective. Additionally, the reproducibility of this system was also investigated by treatment of four independent electrodes toward the same Pb^{2+} concentration (10 nM). The relative standard deviation (RSD) of four measurements is 5.87%. Although the RSD is relatively high owing to the interaction using electrostatic adsorption, the system yet has an acceptable reproducibility.

The practicality of the assay

To test the practicality of proposed method, recovery experiments for drinking water acquired from the tap in our laboratory with different Pb^{2+} concentrations (0.5, 10, 100 nM) were carried out. The corresponding results are displayed in Table 2. The recoveries and relative standard deviations (RSDs) are ranged from 96.2%–103.5% and 4.3%–5.2%, respectively, suggesting that the proposed biosensor hold a potential application in detection of Pb^{2+} in drinking water. Additionally, the tap water samples containing defined Pb^{2+} concentration by atomic absorption spectrometry (AAS) were also studied by proposed biosensor. The results in Table 3

shows that the experimental data obtained by the proposed biosensor were approximate to that of AAS, further suggesting potential application of proposed biosensor in detection of Pb^{2+} in drinking water.

Conclusions

An effective way was proposed to detect Pb^{2+} by combining ion-dependent split DNAzyme and template-free DNA extension reaction. The proposed EC biosensor had two features: First, the substantial primers produced by the cycle of Pb^{2+}-dependent split DNAzyme triggered the temple-free DNA extension reaction, avoiding the strict base pairing to make the detection system became simply. Second, the Pb^{2+}-dependent split DNAzyme avoided the usage of enzyme label, providing a simple and sensitive strategy for Pb^{2+} analysis.

Acknowledgements This work was supported by the Fundamental Research Funds for the Central Universities (XDJK2019B022, SWU117045), the Chongqing Research Program of Basic Research and Frontier Technology (cstc2018jcyjA0797) and the national key research and development plan of China (2018YFD0800600).

References

1. Sun J, Luo L (2018) Subcellular distribution and chemical forms of Pb in corn: strategies underlying tolerance in Pb stress. J Agric Food Chem 66(26):6675–6682
2. Zhu H, Tan X, Tan L, Zhang H, Liu H, Fang M, Wang X (2018) Magnetic porous polymers prepared via high internal phase emulsions for efficient removal of Pb^{2+} and Cd^{2+}. ACS Sustain Chem Eng 6(4):5206–5213
3. Tang DP, Xia BY, Tang Y, Zhang J, Zhou Q (2019) Metal-ion-induced DNAzyme on magnetic beads for detection of lead (II) by using rolling circle amplification, glucose oxidase, and readout of pH changes. Microchim Acta 186(5):318–326
4. Islam E, Liu D, Li T, Yang X, Jin X, Khan MA, Mahmood Q, Hayat Y, Imtiaz M (2011) Effect of Pb toxicity on the growth and physiology of two ecotypes of Elsholtzia argyi and its alleviation by Zn. Environ Toxicol 26(4):403–416
5. Lo W, Chua H, Lam KH, Bi SP (1999) A comparative investigation on the biosorption of lead by filamentous fungal biomass. Chemosphere 39(15):2723–2736
6. Huang MR, Ding YB, Li XG (2014) Combinatorial screening of potentiometric Pb (II) sensors from polysulfoaminoanthraquinone solid ionophore. ACS Comb Sci 16(3):128–138
7. Zhu CH, Zhu WY, Xu L, Zhou XM (2019) A label-free electrochemical aptasensor based on magnetic biocomposites with Pb^{2+}-dependent DNAzyme for the detection of thrombin. Anal Chim Acta 1047:21–27
8. Shi Y, Wang HY, Jiang XX, Sun B, Song B, Su YY, He Y (2016) Ultrasensitive, specific, recyclable, and reproducible detection of lead ions in real systems through a polyadenine-assisted, surface-enhanced Raman scattering silicon chip. Anal Chem 88(7):3723–3729
9. Deng DD, Yang H, Liu C, Zhao K, Li JG, Deng AP (2019) Ultrasensitive detection of diclofenac in water samples by a novel surface-enhanced Raman scattering (SERS)-based immunochromatographic assay using AgMBA@ SiO_2-Ab as immunoprobe. Sensor Actuat B-Chem 283:563–570
10. Shi XH, Gu W, Peng WD, Li BY, Chen NN, Zhao K, Xian YZ (2014) Sensitive Pb^{2+} probe based on the fluorescence quenching by graphene oxide and enhancement of the leaching of gold nanoparticles. ACS Appl Mater Inter 6(4):2568–2575
11. Annadhasan M, Muthukumarasamyvel T, Sankar Babu VR, Rajendiran N (2014) Green synthesized silver and gold nanoparticles for colorimetric detection of Hg^{2+}, Pb^{2+}, and Mn^{2+} in aqueous medium. ACS Sustain Chem Eng 2(4):887–896
12. Lei YM, Huang WX, Zhao M, Chai YQ, Yuan R, Zhuo Y (2015) Electrochemiluminescence resonance energy transfer system: mechanism and application in ratiometric aptasensor for lead ion. Anal Chem 87(15):7787–7794
13. Kashi MB, Silva SM, Yang Y, Goncales VR, Parker SG, Barfidokht A, Ciampi S, Gooding JJ (2017) Light-activated electrochemistry without surface-bound redox species. Electrochim Acta 251:250–255
14. Sun QW, Wang JK, Tang MH, Huang LM, Zhang ZY, Liu C, Lu XH, Hunter KW, Chen GS (2017) A new electrochemical system based on a flow-field shaped solid electrode and 3D-printed thin-layer flow cell: detection of Pb^{2+} ions by continuous flow accumulation square-wave anodic stripping voltammetry. Anal Chem 89(9):5024–5029
15. Hu Q, Kong JM, Han DX, Niu L, Zhang XL (2019) Electrochemical DNA Biosensing via Electrochemically Controlled Reversible Addition–Fragmentation Chain Transfer Polymerization. ACS Sens 4(1):235–241
16. Ma L, Guo T, Pan SL, Zhang YH (2018) A fluorometric aptasensor for patulin based on the use of magnetized graphene oxide and DNase I-assisted target recycling amplification. Microchim Acta 185(10):487–492
17. Han C, Li RG, Li H, Liu S, Xu CG, Wang JF, Wang Y, Huang JD (2017) Ultrasensitive voltammetric determination of kanamycin using a target-triggered cascade enzymatic recycling couple along with DNAzyme amplification. Microchim Acta 184(8):2941–2948
18. Zhang JP, Chao LC, Zhi X, Ramon GR, Liu YL, Zhang CL, Pan F, Cui DX (2016) Hairpin DNA-templated silver nanoclusters as novel beacons in strand displacement amplification for microRNA detection. Anal Chem 88(2):1294–1302
19. Li MX, Xu CH, Zhang N, Qian GS, Zhao WW, Xu JJ, Chen HY (2018) Exploration of the kinetics of toehold-mediated strand displacement via plasmon rulers. ACS Nano 12(7):3341–3350
20. Chen F, Zhao Y, Fan CH, Zhao YX (2015) Mismatch extension of DNA polymerases and high-accuracy single nucleotide polymorphism diagnostics by gold nanoparticle-improved isothermal amplification. Anal Chem 87(17):8718–8723
21. Yao Q, Wang YQ, Wang J, Chen SM, Liu HY, Jiang ZR, Zhang XE, Liu SM, Yuan Q, Zhou X (2018) An ultrasensitive diagnostic biochip based on biomimetic periodic nanostructure-assisted rolling circle amplification. ACS Nano 12(7):6777–6783
22. Zhao WA, Ali MM, Brook MA, Li YF (2008) Rolling circle amplification: applications in nanotechnology and biodetection with functional nucleic acids. Angew Chem Int Ed 47:6330–6337
23. Chen Y, Xu J, Su J, Xiang Y, Yuan R, Chai YQ (2012) In situ hybridization chain reaction amplification for universal and highly sensitive electrochemiluminescent detection of DNA. Anal Chem 84(18):7750–7755
24. He Z, Cai Y, Yang Z, Li P, Lei H, Liu W, Liu Y (2019) A dual-signal readout enzyme-free immunosensor based on hybridization chain reaction-assisted formation of copper nanoparticles for the detection of microcystin-LR. Biosens Bioelectron 126:151–159
25. Cao HM, Zhou X, Zeng Y (2019) Microfluidic exponential rolling circle amplification for sensitive microRNA detection directly from biological samples. Sensor Actuat B-Chem 279:447–457

26. Reid MS, Rebecca E, Paliwoda RE, Zhang HQ, Le XC (2018) Reduction of background generated from template-template hybridizations in the exponential amplification reaction. Anal Chem 90(18):11033–11039
27. Zhang M, Wang Y, Yuan S, Sun X, Huo B, Bai J, Gao Z (2019) Competitive fluorometric assay for the food toxin T-2 by using DNA-modified silver nanoclusters, aptamer-modified magnetic beads, and exponential isothermal amplification. Microchim Acta 186(4):219–225
28. Yu CY, Yin BC, Wang SL, Xu ZG, Ye BC (2014) Improved ligation-mediated PCR method coupled with T7 RNA polymerase for sensitive DNA detection. Anal Chem 86(15):7214–7218
29. Du WF, Ge JH, Li JJ, Tang LJ, Yu RQ, Jiang JH (2019) Single-step, high-specificity detection of single nucleotide mutation by primer-activatable loop-mediated isothermal amplification (PA-LAMP). Anal Chim Acta 1050:132–138
30. Cai S, Jung C, Bhadra S, Ellington A (2018) Phosphorothioated primers lead to loop-mediated isothermal amplification at low temperatures. Anal Chem 90(14):8290–8294
31. Du YC, Cui YX, Li XY, Sun GY, Zhang YP, Tang AN, Kong DM (2018) Terminal deoxynucleotidyl transferase and T7 exonuclease-aided amplification strategy for ultrasensitive detection of uracil-DNA glycosylase. Anal Chem 90(14):8629–8634
32. Yang F, Yang X, Wang YZ, Qin Y, Liu X, Yan XQ, Zou K, Ning Y, Zhang GJ (2014) Template-independent, in situ grown DNA nanotail enabling label-free femtomolar chronocoulometric detection of nucleic acids. Anal Chem 86(23):11905–11912
33. Xie SB, Dong YW, Yuan YL, Chai YQ, Yuan R (2016) Ultrasensitive lipopolysaccharides detection based on doxorubicin conjugated N-(Aminobutyl)-N-(ethylisoluminol) as electrochemiluminescence indicator and self-assembled tetrahedron DNA dendrimers as nanocarriers. Anal Chem 88(10):5218–5224
34. Niu XF, Zhong YB, Chen R, Wang F, Liu YJ, Luo D (2018) A "turn-on" fluorescence sensor for Pb^{2+} detection based on graphene quantum dots and gold nanoparticles. Sensor Actuat B-Chem 255: 1577–1581
35. Wang Y, Wang J, Yang F, Yang XR (2010) Spectrophotometric detection of lead(II) ion using unimolecular peroxidase-like deoxyribozyme. Microchim Acta 171:195–201
36. Chai F, Wang CG, Wang TT, Li L, Su ZM (2010) Colorimetric detection of Pb^{2+} using glutathione functionalized gold nanoparticles. ACS Appl Mater Interfaces 2:1466–1470
37. Lidia M, Crina S, Maria C, Florina P, Marcela CR, Stefan G, Stela P (2017) Electrochemical platform based on nitrogendoped graphene/chitosan nanocomposite for selective Pb^{2+} detection. Nanotechnology 28:114001–1140012
38. Huang ZJ, Chen JM, Luo ZW, Wang XQ, Duan YX (2019) Label-free and enzyme-free colorimetric detection of Pb^{2+} based on RNA cleavage and annealing-accelerated hybridization chain reaction. Anal Chem 917:4806–4813
39. Lu HZ, Xu SF, Liu JQ (2019) One pot generation of blue and red carbon dots in one binary solvent system for dual channel detection of Cr^{3+} and Pb^{2+} based on ion imprinted fluorescence polymers. ACS Sens 4:1917–1924
40. Cui L, Wu J, Li Jie JHX (2015) Electrochemical sensor for lead cation sensitized with a DNA functionalized porphyrinic metal-organic framework. Anal Chem 87:10635–10641
41. Song XL, Wang Y, Liu S, Zhang X, Wang JF, Wang HW, Zhang FF, Yu JH, Huang JD (2019) A triply amplified electrochemical lead(II) sensor by using a DNAzyme and via formation of a DNA-gold nanoparticle network induced by a catalytic hairpin assembly. Microchim Acta 186:559–566
42. Shahdordizadeh M, Yazdian-Robati R, Ansari N, Ramezani M, Abnous K, Taghdisi SM (2018) An aptamer-based colorimetric lead(II) assay based on the use of gold nanoparticles modified with dsDNA and exonuclease I. Microchim Acta 185:151–156
43. Ravikumar A, Panneerselvam P, Radhakrishnan K (2018) Fluorometric determination of lead(II) and mercury(II) based on their interaction with a complex formed between graphene oxide and a DNAzyme. Microchim Acta 185:2–9